APS physics

CHORUS

This is the accepted manuscript made available via CHORUS. The article has been published as:

Photon echoes from an atomic frequency comb affected by population relaxation

Devin Vega and Mingzhen Tian

Phys. Rev. A **98**, 052340 — Published 26 November 2018

DOI: 10.1103/PhysRevA.98.052340

Photon Echoes from an Atomic Frequency Comb Affected by Population Relaxation

Devin Vega and Mingzhen Tian

Department of Physics and Astronomy, Quantum Materials Center,

George Mason University, Fairfax, VA 22030

Abstract: The atomic frequency comb (AFC) is a promising approach for quantum memory, yet creating an ideal AFC only in the ground state population remains a challenge. We studied an imperfect AFC initially created in the population inversion between the excited and ground states and redistributed due to population relaxation in a three-level system where a long-lived metastable state plays a crucial role. A theoretical model has been developed to treat the storage of a weak input pulse and retrieval in the form of a photon echo. By comparing theory with experimental results we have studied the echo efficiency and overall attenuation of an input pulse in the AFC affected by both its initial spectral structure and the population relaxation.

PACS: 03.67.Hk, 42.50.Md, 42.50.Ex, 42.50.Gy.

I. INTRODUCTION

Applications for quantum memories are many fold [1-5]. Quantum repeaters [6-8] and linear optics based quantum computing [9,10], as well as quantum error correction [11], precision metrology [12], and deterministic single photon sources [13] are some of the many applications requiring quantum information storage as a critical component. In the realm of solid state light-matter interfaces, the atomic frequency comb (AFC) protocol has seen significant amounts of research, with recent work demonstrating the potential for high fidelity, high efficiency, multimode storage, and long storage times [14-17]. The creation of an AFC and storage of a photon wave packet in an atomic ensemble is similar to a stimulated photon echo process in a two-level atomic ensemble except the AFC requires a third long-lived metastable state [2]. The atomic population in the ground state is selectively transferred to the meta-stable state by optical pumping, usually through excitation to the excited state followed by relaxation to the metastable level. This leaves the spectral distribution of unexcited atoms in ground state resembling a comb of equally spaced, identical teeth. A photon wave packet encoded with an input quantum state interacts with the AFC, creating a collective atomic coherence whose rephasing process leads to the emission of a delayed copy of the input wave packet in the form of photon echo. The storage time and efficiency is programmed in the AFC by optical pumping either with frequency-chirped pulses or repeated pulse pairs [18,19]. The ideal AFC structure for optimal storage efficiency is

theoretically well-known [14,18], defined by the tooth shape, peak absorption, and finesse of the comb under the condition that the excited state is completely empty and ground state is mostly empty except for the sharp comb teeth. However, achieving the optimal condition remains a challenge due to the nature of the pump/relaxation process of the atomic population in a three-level system.

In an AFC memory, the storage and retrieval process is meant to occur after the excited state population has completely decayed, but before the decay of the atoms from the metastable state back to ground. In practical application, lower and upper bounds on the time window of an AFC memory are set by the lifetimes of the excited and metastable states. Furthermore, the storage efficiency and fidelity vary due to the relaxation of the atomic population which changes the spectral distribution among the three levels. Any residual population in the excited state by the time the input is sent into the AFC will cause noise and low fidelity in the retrieved photon wave packet due to spontaneous emission. At the same time, an elevated population inversion between the excited and ground states boosts echo efficiency due to reduction of reabsorption of the photon echo, or turning the AFC into an amplifier. At the upper bound of the time window, the metastable state population begins to decay back to the ground state. This will cause an overall background population to be added to the AFC, which will result in low memory efficiency. An imperfect pumping or a direct relaxation from the excited to ground states can have a similar effect.

In this paper, we study how the population relaxation in a three-level atomic ensemble affects an imperfectly pumped AFC. In the following section, we present a semi-classical theory that treats the storage and retrieval of a weak classical pulse in AFC. The model includes the population redistribution in the spectral comb after pumping and its impact on the absorption of the input and emission of echo pulses. This will address the case of population in the excited state as well as background in the ground state. We then describe experiments with a Thulium ion ensemble doped in a yttrium aluminum garnet crystal (Tm:YAG) in section III. In section IV, the experimental results are discussed and compared with the theory. We obtained the relaxation parameters, such as lifetimes of the excited and metastable states and branching ratio of the two relaxation paths. We also studied relaxation dynamics, the overall attenuation of a weak pulse propagating through the AFC, and echo efficiency. We conclude in Section V. Appendices A

and B contain the solutions to rate equations and backward propagating photon echoes, respectively.

II. THEORY

Similar to the original AFC protocol in ref [14], we use coupled Maxwell-Bloch equations to describe the interaction of an atomic ensemble and electric fields of the weak pulses near the atomic resonance, including the input and its echoes [20].

$$\dot{\rho}_f(z,\Delta,t) = -i\Omega_f(z,t)w(\Delta) - i\Delta\rho_f(z,\Delta,t) \quad (1)$$

$$\partial_z\Omega_f(z,t) = i\alpha/2\pi\int_{-\infty}^{\infty}\rho_f(z,\Delta,t)d\Delta \quad (2)$$

where ρ_f is the atomic coherence, Ω_f is the Rabi frequency of the weak field, and Δ is the detuning of the atomic resonance from the field frequency. The subscript f denotes the wave packets traveling in the forward direction along z-axis. The uniform absorption coefficient of the initial atomic ensemble is denoted by α. We use the spectral distribution of the atomic population inversion, $w(\Delta)$, between the excited and ground states to represent an AFC. By convention, the population inversion is defined as $w(\Delta) = p_e(\Delta) - p_g(\Delta)$, where $p_{e,g}(\Delta)$ denotes the probability of an atom, resonant at detuning Δ, occupying the excited and ground states, respectively. The protocol in ref [14] assumes $w(\Delta) = -1$ at the teeth peaks and $w(\Delta) = 0$ on the spectrum between teeth. We consider an AFC in a more general form.

$$w(\Delta) = b - (b+1)\xi(\Delta) * d(\Delta). \quad (3)$$

The Dirac comb function $d(\Delta) = \sum_{n=-\infty}^{\infty}\delta(\Delta - n\Gamma)$ is defined by the frequency spacing Γ between the teeth for a larger number of teeth $n >> 1$. A single tooth is described by a positive-valued function $\xi(\Delta)$ with a normalized peak and a width $\gamma < \Gamma$. The convolution $\xi(\Delta) * d(\Delta)$ sets the periodic structure on the spectrum as shown in Fig. 1a. A flat background is denoted by b. Fig 1b and 1c plot AFCs of different background levels. In Fig. 1b, the excited and ground states are equally populated on the spectrum between teeth ($b = 0$ due to $p_e = p_g$). This includes the ideal case described in ref [14], where no atom occupies these states between the teeth, ie. $p_e = p_g = 0$. Fig. 1c illustrates two cases. The maximum (solid line for $b = 1$) and minimum (dashed line for $b = -1$) of background level correspond to a fully occupied excited state ($p_e = 1$) between the teeth and a fully occupied ground state ($p_g = 1$), respectively. The actual

background level falls in the range $-1 \le b \le 1$ depending on the level of initial pumping and the population relaxation, which will be addressed after we solve the equations (1) and (2) based on the general form of the AFC defined in equation (3).

Under the condition that the overall pulse area is much smaller than π, the inversion $w(\Delta)$ is not affected by the field. Equations (1) and (2) lead to a field equation,

$$\partial_z \Omega_f(z,t) = -\alpha/(2\sqrt{2\pi})\{[1+sign(t)]W(t)\} * \Omega_f(z,t) \quad (4)$$

where $W(t) = b\delta(t) - (b+1)X(t)\sum_{n=-\infty}^{\infty}\delta(t - 2\pi n/\Gamma)$ and $X(t) = 1/\sqrt{2\pi}\int_{-\infty}^{\infty}\xi(\Delta)e^{-i\Delta t}dt$ are the Fourier transforms of the AFC defined in equation (3) and the single tooth function, respectively.

Equation (4) indicates that the output field peaks periodically at $t = 2n\pi/\Gamma$ for $n = 0,1,2...$ corresponding to the transmitted input pulse, the first order, and higher order photon echoes. Focusing on the first two pulses, input at $t = 0$ and echo at $t = 2\pi/\Gamma$, we solved for the peak amplitudes of the output from an atomic ensemble of length L.

$$\Omega_{f0} = \Omega_0 e^{g/2} \quad (5)$$

$$\Omega_{f1} = \Omega_0 e^{g/2}\alpha L(b+1)X_1/\Gamma \quad (6)$$

where Ω_0 is the peak amplitude of input pulse. The average gain/attenuation in an atomic ensemble with a peak absorption length of αL is represented by $g = \alpha L[b-(b+1)X_0/\Gamma]$, where X_0 and X_1 denote the Fourier components $X_n = \sqrt{2\pi}X(t = 2\pi n/\Gamma)$ for $n = 0$ and 1. Equation (5) shows that a positive (negative) valued g corresponds to an overall amplification (absorption) of a pulse passing through the atomic ensemble.

The transmittance of input pulse and the echo efficiency are defined, respectively,

$$\eta_{f0} = (\Omega_{f0}/\Omega_0)^2 = e^g \quad (7)$$

$$\eta_{f1} = (\Omega_{f1}/\Omega_0)^2 = [\alpha L(b+1)X_1/\Gamma]^2 e^g \quad (8)$$

The intensities of transmitted input ${\Omega_{f0}}^2$ and generated echo ${\Omega_{f1}}^2$ on the output side are compared with the intensity of input pulse ${\Omega_0}^2$. In an AFC made of the ground state population as shown in Fig. 1b, the ensemble is absorptive ($g < 0$), which leads to $\eta_{f0}, \eta_{f1} < 1$ [14].

However, both ratios can be larger than unity when significant population in the excited state results in amplification in the ensemble ($g > 0$), such as the case shown as a solid line in Fig. 1c.

So far, we have assumed that $w(\Delta)$ is a time–independent function during the time span from the input pulse to its first echo, which is generally valid provided the relaxation process is much longer than the coherence time in the atomic ensemble. However, a time delay T_d between the AFC's creation and the input pulse can cause significant population redistribution in a three-level system (as shown in Fig. 2a) due to population relaxation. In order to study the relaxation process, rate equations are solved in Appendix A. According to equation (A3), during delay T_d, the AFC's background changes from an initial value b_0 to

$$b = (b_0 + 1)(\beta + 1)/2 - 1 \tag{9}$$

where the decay factor is defined as

$$\beta = 2e^{-T_d/T_e} + \lambda T_m (e^{-T_d/T_e} - e^{-T_d/T_m})/(T_e - T_m) - 1 \tag{10}$$

T_e and T_m are the lifetimes of the excited and metastable states, respectively, and λ is the branching fraction of the $|e\rangle \to |m\rangle$ transition. The β value starts from 1 at $T_d = 0$ and decreases to -1 as $T_d \to \infty$. According to equation (9), the background varies from b_0 to -1, which corresponds to the inversion spectrum around a comb tooth starting from the initial structure $b_0 - (b_0 + 1)\xi(\Delta)$ and reducing to a flat value at -1, shown as the dashed line in Fig.1c.

In an ideal AFC the excited state is unoccupied, such that the ground state population forms the teeth, with all other atoms pumped to the metastable level, shown as in Fig. 1b. This requires both $b_0 = 1$ and $\beta = 0$ be satisfied. The first of these conditions means that all atoms outside the teeth should be initially excited. The second requires that the population relaxation in the three-level system satisfies $T_1 << T_d << T_m$ and all excited atoms should decay to the metastable state ($\lambda = 1$). When these conditions are satisfied, the AFC has zero background, $b = 0$ [according to equations (9) and (10)] and $g = -\alpha L X_0 / \Gamma$ turns into an average attenuation. This is consistent with the results in ref [14].

According to Equations (5) through (10), we can study pulse propagation and echo emission varying with the relaxation time T_d in an AFC consisting of both ground and excited state populations. Both transmittance and echo efficiency depend on the initial inversion b_0, and the

decay factor β in addition to the above-mentioned AFC parameters, such as the tooth shape, peak absorption, and finesse. We can also calculate the ratio of the peak power of the echo to that of the transmitted input pulse, which turns out to be a simple function of the decay factor β.

$$R = (\Omega_{f1} / \Omega_{f0})^2 = [\alpha L X_1 (b_0 + 1) / (2\Gamma)]^2 (\beta + 1)^2 \quad (11)$$

This provides a reliable way to measure the lifetimes and branching ratio of the three-level atomic ensemble and verify our theory with experiment. In the next two sections we will discuss the experiment setup and results for forward propagating echoes that match the theory.

We also note that the first-order echo Ω_{b1} propagating in the opposite direct of the input can be calculated in a similar way as shown in Appendix B with echo efficiency expressed by

$$\eta_{b1} = [\alpha L X_1 (\beta + 1) / \Gamma]^2 [1 - e^g) / g]^2 \quad (12)$$

III. EXPERIMENT

Fig. 2b shows a sketch of the main components in the experiment setup. The sample was a yttrium aluminum garnet crystal doped with 0.5 at.% thulium ions (Tm^{3+}), cooled to ~4 Kelvin. The optical pumping, input pulse, and photon echo are all near resonance with the thulium $^3H_6$ (ground) to $^3H_4$ (excited state) transition at 793.38 nm while $^3F_4$ serves as the metastable state. The lifetimes of the excited and metastable states were previously estimated to be sub-milliseconds and tens of milliseconds, respectively [21]. The laser source was a Toptica continuous wave diode laser, amplitude modulated and/or frequency-chirped with an acousto-optic modulator driven by a Tektronix 7052 arbitrary waveform generator. The laser field is polarized along the crystal's [111] axis in order to achieve the same projected atomic dipole moment from all interacting dipole sites [22]. Another Tm^{+3}:YAG crystal with 0.1 at.% doping in the same sample chamber was used to provide optical feedback for frequency stabilization [23,24]. The feedback along this second beam branch resulted in a laser linewidth of a few tens of kilohertz at most. The optical nutation signal shows the laser frequency stable for a few hundred microseconds. The coherence time of the thulium ensemble was measured to be 25 μs [25].

A population inversion in the shape of an AFC with 7 teeth was created with a sequence of eight adiabatic WURST pulses [26] by linear chirping of the laser frequency across 40 MHz. Each WURST pulse was 20 μs long, burning a spectral hole of ~4 MHz wide with 5 MHz spacing. The amplitude and frequency of the WURST pulses programmed in the AWG is plotted in Fig. 3a. A transmission spectrum of the AFC, shown in Fig. 3b, was measured by linearly

scanning the frequency of an 800 μs -long weak pulse across 40 MHz. The reduction of the transmission with the scanning time indicates the population inversion decaying while being probed.

The input pulse to be stored was a low intensity Gaussian pulse with frequency at the comb's center. The peak power was fixed and measured. The pulse duration was set so that its full width at half maximum (FWHM) of the power spectrum was either 5.3 MHz or 9.6 MHz, which span roughly 1 or 2 times the comb's spacing. The echo was emitted in the forward direction with a delay of 0.2 μs. We varied the time delay, T_d , between the creation of the comb center and Gaussian input pulse and recorded the transmitted input and its echo. An example at $T_d = 130\mu s$ is plotted in Fig. 3c.

IV RESULTS AND DISCUSSION

We first study the population relaxation in the three-level system using experimental data and equation (11). The measured ratio of the echo intensity over transmitted input is plotted (dots) in Fig. 4. The data points for both probe widths (diamonds for 5.3 MHz and triangles for 9.6 MHz) follow the same decay trend. Fitting the data points to equation (11) (solid curve) yields the lifetimes, $T_1 = 0.5ms$, $T_m = 14ms$, and branching fraction $\lambda = 0.9$ with corresponding uncertainties at 2%, 18%, and 3%, respectively. A large uncertainty in T_m is expected because the range of time delay covered by the experimental data is shorter than the metastable lifetime. With these parameters, the value of the decay factor β was calculated at every T_d value.

Next, we estimate the initial comb structure, including the peak absorption αL , inversion b_0 , and finesse Γ/γ . The gain/attenuation factors $g = \ln(\eta_0)$ defined in equation (7) for experimental data points are plotted against β in Fig. 5. According to equation (9), the factor g is a simple linear function of β , $g = \beta(g_0 + \alpha L)/2 + (g_0 - \alpha L)/2$, where $g_0 = \alpha L[b_0 - (b_0 + 1)X_0/\Gamma]$ is the initial value immediately after pumping. The experimental data (dots) for 5.3 MHz and 9.6 MHz in Fig. 5 confirm the linear relation. Fitting the linear function to the two sets of experimental data, we have a mean value of the slope at 2.51 and intercept at -2.05. From these we calculated the peak absorption length, $\alpha L = 4.56$, and an average initial gain, $g_0 = 0.46$. Together with the factor $[\alpha L(b_0 + 1)X_1/\Gamma]^2 = 0.55$ obtained from the fitting in Fig. 4, we can estimate the initial inversion b_0 and the comb's finesse Γ/γ . Assuming a Gaussian-shaped tooth function, $\xi(\Delta) = e^{-4\ln 2\Delta^2/\gamma^2}$,

the Fourier components are calculated to be $X_0 = \sqrt{\pi/(4\ln 2)}\gamma \approx 1.06\gamma$ and $X_1 \approx 1.06\gamma e^{-3.56(\gamma/\Gamma)^2}$, respectively. From the fitting parameters above, we estimate an initial inversion of $b_0 \approx 0.5$, which means 75% of the population between the teeth is initially inverted to the excited state by the WUSRT pulse. The AFC's finesse is estimated to be $\Gamma/\gamma = 4$. These values are similar for square-shaped teeth. The comb's teeth in the experiment are in a shape between Gaussian and square.

The measured transmittance of input and efficiency of the first order echo as a function of delay time are plotted as the dots in Fig. 6. The solid curves are the theoretical results calculated according to equations (7) and (8). The initially inverted AFC is created at $T_d = 0$. At $T_d = 2\ ms$, about four times the excited state lifetime, ~99% of the excited population has decayed from the excited state to the metastable and ground states at a 9:1 ratio. Within the time span in the plot, the population in the metastable level has not significantly decayed to the ground state. The theoretical curves show a transmittance greater than 1 at short delay. This is due to the positive average inversion in the initial AFC, in which the average population in the excited state is greater than that of the ground state and causes amplification of a pulse propagating through it. Both theoretical and measured data show greater than unit efficiency in the first order echo at short delay. However, the high echo efficiency is not simply due to an amplification effect since it is greater than the transmittance initially and does not follow the same decay curve. In fact, the measured data at the few short delays between 130 to 190 μs shows more than 100% echo efficiency in an overall absorptive AFC. Our experimental results also indicate that the transmittance and echo efficiency do not depend on the input pulse's bandwidth as long as it is narrower than the overall AFC bandwidth.

In an ideal AFC, the backward configuration allows up to 100% memory efficiency while the maximum for forward retrieval is ~54% [14]. On the other hand, if an AFC is imperfect, the difference between the two may become insignificant. The backward echo efficiency calculated with equation (12) under our experimental conditions is plotted in Fig. 6 as the dashed line. Both configurations start off at almost the same efficiency at more than 300% and decay to a few percent after the excited state is almost empty at $T_d = 2\ ms$.

V. CONCLUSION

We have studied the dynamics of an imperfect AFC by developing a theoretical model and comparing it with experimental results. The semi-classical theory can treat the storage/retrieval as a photon echo process in an AFC made of atomic populations both in ground and excited states. The model allows us to calculate the echo efficiency as a function of the population relaxation time in a three-level system after the initial pumping, as well as monitoring the overall amplification/attenuation of a pulse propagating through the AFC. Using a thulium ensemble doped in a YAG crystal, we measured echo efficiency and transmittance of an input pulse as a function of the time delay between the creation of the AFC and the input pulse. Both agree with the theory. Fitting experimental data to the theory also provides a reliable way to measure the relaxation parameters, such as the lifetimes and the relaxation branching ratio. Comparing the experiment to theory, we can also extract information about the AFC structure, such as the absorption length before optical pumping, the level of population inversion between the teeth, and the finesse. The method developed in this paper is applicable to the AFC in a general three-level system. For the sample used in our experiment, the echo efficiency decayed from ~150% at 130 μs to a few percent at four times the excited state lifetime. We note that in some delay range (130 μs to 190 μs in our experiment) shorter than the excited state lifetime, more than unit echo efficiency can happen in an overall absorptive AFC where the majority of the relevant atomic population is in the ground state. The population distribution in the excited state and its contribution to the quantum noise and echo efficiency in this region will be interesting questions for future work.

ACKNOWLEDGMENTS

The authors wish to acknowledge the grant support from the National Science Foundation (PHY-1212360).

APPENDIX A: RATE EQUATIONS

The atomic population in a three-level system as shown in figure 2a decays after pumping. The population rates of change are determined by the excited and the metastable state lifetimes T_1 and T_m, and the excited-to-metastable relaxation branching fraction λ in the following rate equations.

$$\begin{aligned} \dot{p}_e &= -p_e / T_1 \\ \dot{p}_m &= -p_m / T_m + p_e \lambda / T_1 \\ \dot{p}_g &= p_e (1-\lambda) / T_1 + p_m / T_m \end{aligned} \tag{A1}$$

The solutions to these equations give the populations at time T_d after pumping.

$$\begin{aligned} p_e &= p_{e0}e^{-T_d/T_e} \\ p_m &= \lambda p_{e0}(e^{-T_d/T_m} - e^{-T_d/T_e})T_m/(T_m - T_e) \\ p_g &= p_{g0} + p_{e0} - p_{e0}e^{-T_d/T_e} - \lambda\rho_{e0}(e^{-T_d/T_m} - e^{-T_d/T_e})T_m/(T_m - T_e) \end{aligned} \quad \text{(A2)}$$

Where p_{e0} and p_{g0} are the excited and ground state population right after the pumping. The metastable state is unoccupied initially. The population inversion at T_d can be calculated as,

$$p_e - p_g = [(p_{e0} - p_{g0}) + 1][2e^{-T_d/T_1} + \lambda(e^{-T_d/T_1} - e^{-T_d/T_m})T_m/(T_1 - T_m)]/2 - 1 \quad \text{(A3)}$$

APPENDIX B: BACKWARD PHOTON ECHO

According to ref [14], the photon echo from an AFC can be made to propagate in the opposite direction of the input wave packet. The equations describing the atomic coherence ρ_b and propagating field Ω_b are similar to equations (1) and (2) except for a minus sign in the second equation due to the echo travelling in the $-z$ direction.

$$\dot{\rho}_b(z,\Delta,t) = -i\Omega_b(z,t)w(\Delta) - i\Delta\rho_b(z,\Delta,t) \quad \text{(B1)}$$

$$\partial_z\Omega_b(z,t) = -i\alpha/(2\pi)\int_{-\infty}^{\infty}\rho_b(z,\Delta,t)d\Delta \quad \text{(B2)}$$

After Fourier transform of the AFC in $w(\Delta)$, the field equation becomes

$$\partial_z\Omega_b(z,t) = \alpha/(2\sqrt{2\pi})\{[1 + sign(t)]W(t)\} * \Omega_b(z,t) \quad \text{(B3)}$$

It should be noted that equation (B3) is valid for echo pulses centered at $t = 2\pi n/\Gamma$ for integer numbers $n \geq 1$. The input pulse centered at $t = 0$ entered the ensemble at $z = 0$ still obeys equation (4) and can be solved for a location z inside the ensemble as

$$\Omega_{f0}(z) = \Omega_0 e^{gz/2L} \quad \text{(B4)}$$

Setting $t = 2\pi/\Gamma$, the equation for the amplitude of first order echo becomes

$$\frac{d\Omega_{b1}(z)}{dz} = -\frac{g}{2L}\Omega_{b1}(z) + \frac{\alpha}{\Gamma}X_1(\beta + 1)\Omega_{f0}(z) \quad \text{(B5)}$$

Generated echoes exit the ensemble at $z = 0$. The solution to equation (B5) at the output is

$$\Omega_{b1} = \Omega_0\alpha X_1(\beta + 1)/\Gamma\int_L^0 e^{gz/L}dz = \Omega_0\alpha L X_1(\beta + 1)(1 - e^g)/(g\Gamma) \quad \text{(B6)}$$

References:

[1] K. Heshami, D. G. England, P. C. Humphreys, P. J. Bustard, V. M. Acosta, J. Nunn, and B. J. Sussman, J. Mod. Opt. **63**, 2005 (2016).

[2] C. Simon, et. al. Eur. Phys J. D **58**, 1 (2010).

[3] A. I. Lvovsky, B. C. Sanders, W. Tittel, Nat. Photonics **3**, 706 (2009).

[4] W. Tittel, M. Afzelius, T. Chanelière, R. L. Cone, S. Kröll, S. A. Moiseev, and M. Sellars, Laser & Photon. Rev. **4**, 244 (2010).

[5] G. Brennen, E. Giacobino, and C. Simon, New J. Phys. **17**, 050201 (2015); F. Bussières, N. Sangouard, M. Afzelius, H. de Riedmantten, C. Simon, and W. Tittle, J. Mod, Opt. **60**, 1519 (2013).

[6] H.-J. Briegel, W. Dür, J.I. Cirac, and P. Zoller, Phys. Rev. Lett. **81**, 5932 (1998).

[7] L.-M. Duan, M. D. Lukin, J. I. Cirac, and P. Zoller, Nature (London) **414**, 413 (2001)

[8] N. Sangouard, C. Simon, H. de Riedmatten, and N. Gisin, Rev. Mod. Phys. **83**, 33 (2011)

[9] E. Knill, R. Laflamme, and G.J. Milburn, Nature **409**, 46 (2001)

[10] P. Kok, W.J. Munro, K. Nemoto, T.C. Ralph, J.P. Dowling, and G.J. Milburn, Rev. Mod. Phys. **79**, 135-174 (2007).

[11] J. R. Wootton, J. Mod. Opt. **59**, 171 (2012).

[12] J. Appel et al., Proc. Nat. Acad. Sci. Am. **106**, 10960 (2009).

[13] S. Chen, Y.A. Chen, T. Strassel, Z._S. Yuan, B. Zhao, J. Schmiedmayer, and J.-W. Pan. Phys. Rev. Lett. **97**, 173004 (2006).

[14] M. Afzelius, C. Simon, H. de Riedmatten, and N. Gisin, Phys. Rev. A **79**, 1 (2009).

[15] M. Bonarota, J.-L. Le Gouët, and T. Chanelière, New J. Phys. **13**, 013013 (2011).

[16] M. Sabooni, Q. Li, S. Kröll, and L. Rippe Phys. Rev. Lett. **110**, 133604 (2013).

[17] J. Jin, E. Saglamyurek, M. L. G. Puigibert, V. Verma, F. Marsili, S. W. Nam, D. Oblak, and W. Tittel, Phys. Rev. Lett. **115**, 140501 (2015).

[18] M. Bonarota, J. Ruggiero, J.-L. Le Gouët, and T. Chanelière, Phys. Rev. A **81**, 033803 (2010).

[19] A. Amari, A. Walther, M. Sabooni, M. Huang, S. Kröll, M. Afzelius, I. Usmani, B. Lauritzen, N. Sangouard, H. de Riedmatten, and N. Gisin. J. Lumin. **130**, 1579 (2010).

[20] R. L. Shoemaker, *Laser and Coherence Spectroscopy* (Plenum, New York, 1978).

[21] R. M. Macfarlane, Opt. Lett. **18**, 1958 (1993).

[22] Y. Sun, G. M. Wang, R. L. Cone, R. W. Equall, and M. J. M. Leask, Phys. Rev. B **62**, 15443 (2000).

[23] J. W. Tay, W. G. Farr, P. M. Ledingham, D. Korystov, and J. J. Longdell, Phys. Rev. A **87**, 63824 (2013).
[24] C. Thiel, R, Cone, and T. Böttger, J. Lumin. **152**, 84-87 (2014).
[25] D. S. Vega, P. B. Rambow, and M. Tian, J. Opt. Soc. Am. B **35**, 1374 (2018)
[26] E. Kupce and R. Freeman, J. Magn. Reson. Ser. A **115**, 273 (1995); 299, **118** (1996); L. A. O'Dell Solid. State Nucl. Magn. Reson. **55-56**, 28 (2013).

Captions:

(color online) Fig. 1 (a). Squared function as an example of a single tooth $\xi(\Delta)$, Dirac delta function $d(\Delta)$, and convolution $d(\Delta)\otimes\xi(\Delta)$. (b). Population inversion $w(\Delta)$ with a peak value of -1 and background $b=0$. (c). AFC with a peak value of -1 and background at maximum ($b=1$) and minimum ($b=-1$).

(color online) Fig. 2 (a). Three-level system. T_e: excited state lifetime; T_m: metastable state lifetime; λ: $|e\rangle\rightarrow|m\rangle$ relaxation branching fraction. (b) Sketch of experiment setup. AOM: acousto-optical modulator; WM: wavelength meter; F-P: Fabry-Perot spectrum analyzer. Two crystals are cooled to ~4 Kelvin. Two optical isolators various beam splitters and mirrors make an experiment path ending at a photo detector, an optical feedback loop for frequency-stabilization, and a monitoring port leading to the WM and F-P.

(color online) Fig. 3 (a). The amplitude and frequency of eight WURST pulses (20 μs each). (b) Transmission of an 800 μs-long pulse from a linear frequency chirp of 40 MHz centered on the AFC. (c) Transmitted input pulse and echo of 5.2 MHz and 9.6 MHz bandwidth.

(color online) Fig. 4. Measured ratio (R) of the echo power to the transmitted input as a function of delay time (T_d) for 5.2 MHz (diamonds) and 9.6 MHz bandwidth (triangles), and fitting to theory (solid curve).

(color online) Fig. 5 Transmittance for 5.2 MHz (diamonds) and 9.6 MHz (triangles) input pulses and their fitting to linear functions.

(color online) Fig. 6. Comparison of measured values with theory. Circles: measured transmittance of input pulse; Squares: measured efficiency of forward propagating echo; solid line: corresponding theoretical curves; Dashed line: theoretical efficiency of backward propagating echo.

Fig. 1

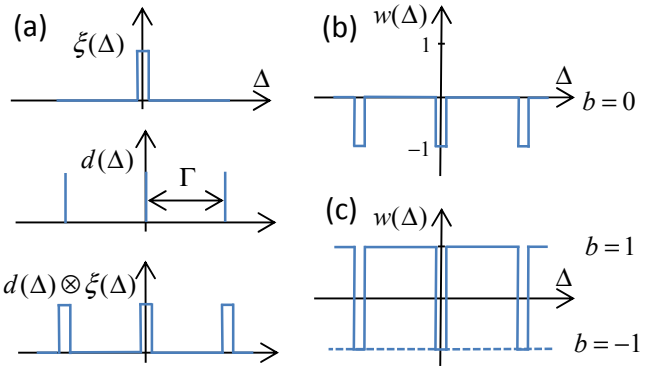
(a)
$\xi(\Delta)$
Δ
$d(\Delta)$
Γ
$d(\Delta)\otimes\xi(\Delta)$
(b)
$w(\Delta)$
1
-1
Δ
$b=0$
(c)
$w(\Delta)$
$b=1$
Δ
$b=-1$

Fig.2

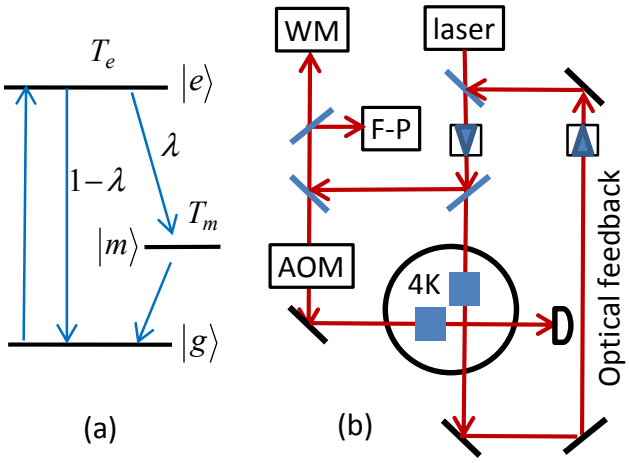
T_e
$|e\rangle$
λ
$1-\lambda$
T_m
$|m\rangle$
$|g\rangle$
(a)
WM
laser
F-P
AOM
4K
D
Optical feedback
(b)

Fig.3

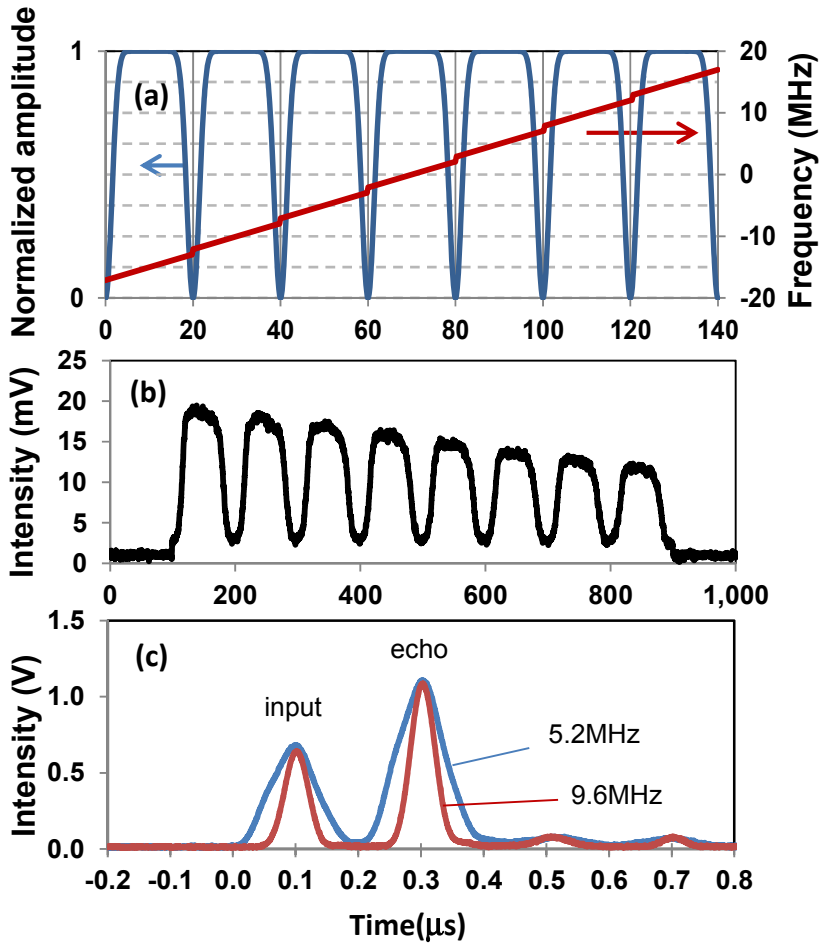
(a)
Normalized amplitude
Frequency (MHz)
1
0
20
10
0
-10
-20
0
20
40
60
80
100
120
140
(b)
Intensity (mV)
25
20
15
10
5
0
0
200
400
600
800
1,000
(c)
Intensity (V)
1.5
1.0
0.5
0.0
input
echo
5.2MHz
9.6MHz
-0.2
-0.1
0.0
0.1
0.2
0.3
0.4
0.5
0.6
0.7
0.8
Time(μs)

Fig.4

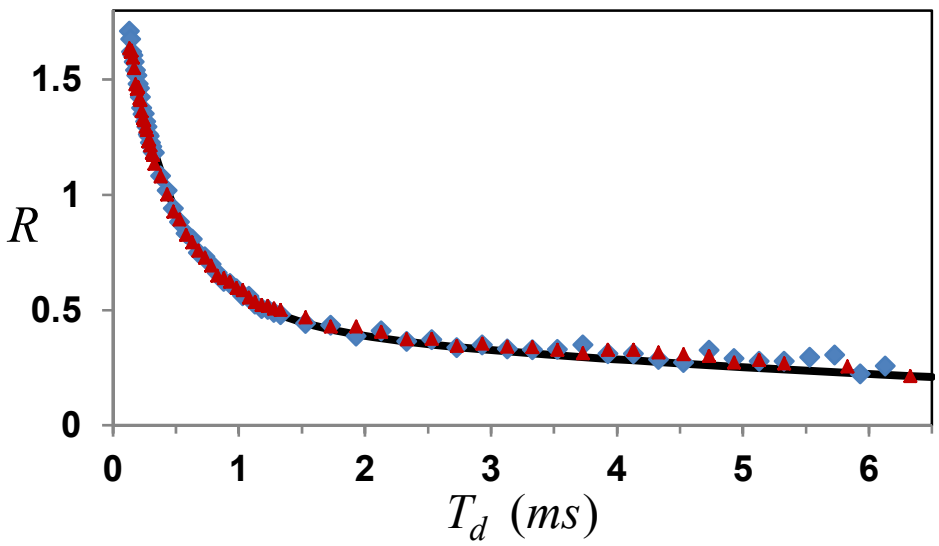

Fig. 5

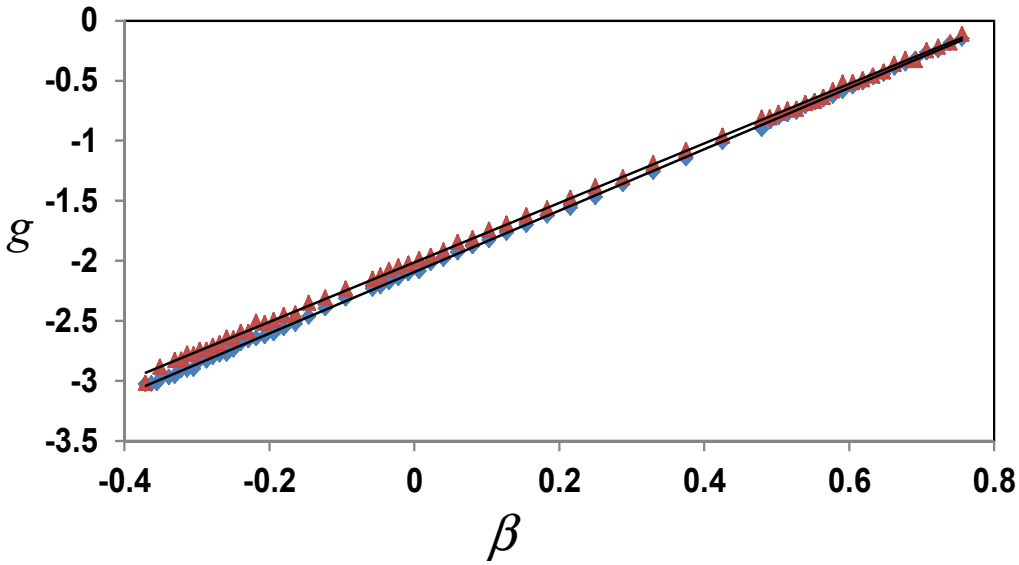

Fig. 6

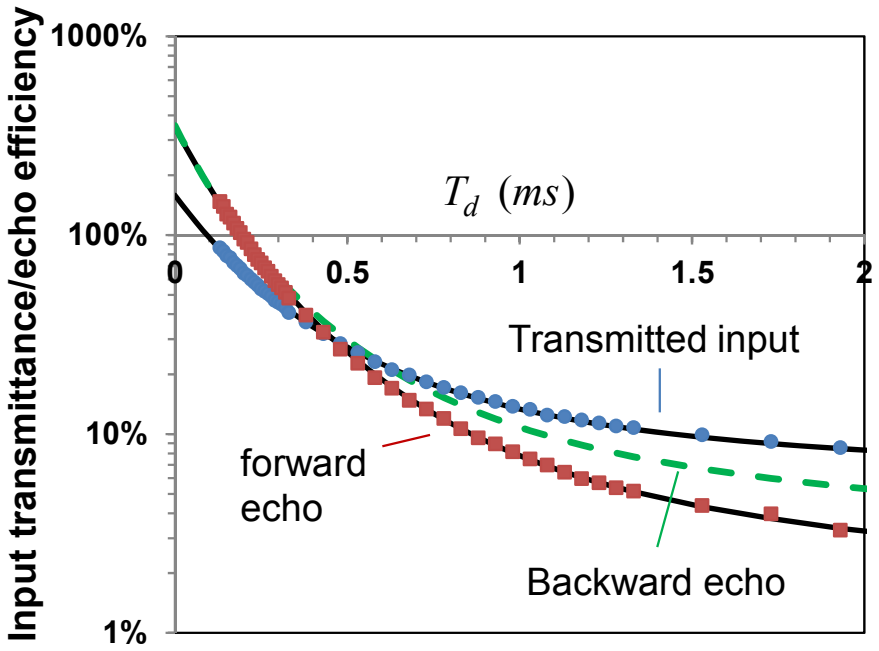
Input transmittance/echo efficiency
1000%
100%
10%
1%
0
0.5
1
1.5
2
T_d (ms)
Transmitted input
forward
echo
Backward echo